# Metallaheteroborane Chemistry. Part 11.[1] Selective Syntheses of the Palladium Heteroborane Complexes [2,2-$(PR_3)_2$-*closo*-2,1-$PdEB_{10}H_{10}$] ($R_3$ = $Ph_3$, $MePh_2$ or $Me_2Ph$; E = Se or Te) and [2-X-2-$(PPh_3)$-*closo*-2,1-$PdTeB_{10}H_9(PPh_3)$] (X = Cl, Br, I, CN, SCN or $O_2CMe$)†

**George Ferguson,*[a] John F. Gallagher,[a] Marguerite McGrath,[b] James P. Sheehan,[b] Trevor R. Spalding*[b] and John D. Kennedy[c]**

[a] *Chemistry Department, University of Guelph, Guelph, Ontario N1G 2W1, Canada*

[b] *Chemistry Department, University College, Cork, Ireland*

[c] *School of Chemistry, University of Leeds, Leeds LS2 9JT, UK*

Reaction of $[PdCl_2(PR_3)_2]$ ($R_3$ = $Ph_3$, $MePh_2$ or $Me_2Ph$) with the *nido*-$[7\text{-}EB_{10}H_{11}]^-$ anions (E = Se or Te) in tetrahydrofuran (thf) at ambient temperature affords twelve-vertex [2,2-$(PR_3)_2$-*closo*-2,1-$PdEB_{10}H_{10}$] complexes selectively in yields ranging from 16 (E = Se, R = Ph) to 82% (E = Te, $R_3$ = $Me_2Ph$). In contrast, the reaction between $[PdX_2(PPh_3)_2]$ (X = Cl or I) and $[7\text{-}TeB_{10}H_{11}]^-$ in refluxing toluene affords only [2-X-2-$(PPh_3)$-*closo*-2,1-$PdTeB_{10}H_9(PPh_3)$] in 39 and 95% yields respectively. Further reactions of [2-I-2-$(PPh_3)$-*closo*-2,1-$PdTeB_{10}H_9(PPh_3)$] with $Hg^{II}$ salts in thf produce [2-X-2-$(PPh_3)$-*closo*-2,1-$PdTeB_{10}H_9(PPh_3)$] complexes (X = Cl, Br, CN, SCN or $O_2CMe$) in yields from 19 (X = $O_2CMe$) to 96% (X = CN). All complexes were characterised by infrared and NMR spectroscopies. Variable-temperature $^1H\text{-}\{^{31}P\}$ NMR spectroscopy of [2,2-$(PMe_2Ph)_2$-*closo*-2,1-$PdSeB_{10}H_{10}$] shows a metal-to-selenaborane rotational bonding fluxionality with $\Delta G^{\ddagger}_{293}$ = 44.5 kJ $mol^{-1}$. An X-ray diffraction study of [2,2-$(PMe_2Ph)_2$-*closo*-2,1-$PdTeB_{10}H_{10}$] **6** reveals the crystals to be monoclinic, space group $P2_1/n$, with $a$ = 13.110(3), $b$ = 10.498(3), $c$ = 19.561(3) Å, β = 105.44(1)° and $Z$ = 4. A final $R$ factor of 0.023 was calculated for 4579 observed reflections. Principal interatomic distances include Pd–Te 2.6833(2), Pd–B 2.234(3)–2.301(3), Te–B 2.294(4)–2.374(3) and Pd–P 2.3301(7) and 2.3354(8) Å. An X-ray diffraction study of [2-$(O_2CMe)$-2-$(PPh_3)$-*closo*-2,1-$PdTeB_{10}H_9(PPh_3)$] **14** recrystallised from $CH_2Cl_2$–*n*-$C_7H_{14}$ as **14**·0.79$CH_2Cl_2$ shows the crystals to be triclinic, space group $P\bar{1}$ with $a$ = 10.416(2), $b$ = 12.409(2), $c$ = 18.720(4) Å, α = 75.59(2), β = 84.10(2), γ = 70.98(1)° and $Z$ = 2. The final $R$ factor is 0.035 for 6472 observed reflections. The acetate ligand is monodentate with Pd–O(1) 2.121(3) Å. Other interatomic distances include Pd–Te 2.6903(4), Pd–P(2) 2.355(1), Pd–B(7) 2.201(5), Pd–B(6) 2.268(4) and B(11)–P(1) 1.942(4) Å.



The continuation of our study of transition-metal complexes of heteroborane ligands [1] has led us to examine the formation and reactions of some palladium compounds of $[EB_{10}H_{10}]^{2-}$ ligands with selenium or tellurium heteroatoms. We have previously reported some bis(phosphine) platinum derivatives containing $[SeB_{10}H_{10}]^{2-}$,[2,3] $[SeB_8H_{10}]^{2-}$[3] or $[TeB_{10}H_{10}]^{2-}$[4] ligands. Part of our interest in metallaheteroboranes is to study the chemistry at the metal atom from both the cluster-to-metal and the metal-to-*exo* cluster points of view. To this end we have developed specific routes to palladium complexes of the general types [2,2-$(PR_3)_2$-*closo*-2,1-$PdEB_{10}H_{10}$] ($R_3$ = $Ph_3$, $MePh_2$ or $Me_2Ph$; E = Se or Te) and [2-X-2-$(PPh_3)$-*closo*-2,1-$PdTeB_{10}H_9(PPh_3)$] (X = Cl or I). Since the Pd–X bond was expected to be substitutionally labile in the $\{PdX(PR_3)\}$ unit, we anticipated it would be possible to synthesise a wide variety of other $\{PdX(PR_3)\}$ complexes. During this work, the structures of [2,2-$(PMe_2Ph)_2$-*closo*-2,1-$PdTeB_{10}H_{10}$] **6** and [2-$(O_2CMe)$-2-$(PPh_3)$-*closo*-2,1-$PdTeB_{10}H_9(PPh_3)$]·0.79$CH_2Cl_2$ **14**·0.79$CH_2Cl_2$ were characterised by X-ray diffraction methods.

## Results and Discussion

Reactions between equimolar amounts of $[PdCl_2(PR_3)_2]$ ($R_3$ = $Ph_3$, $MePh_2$ or $Me_2Ph$) and the *nido* anions $[7\text{-}EB_{10}H_{11}]^-$ (E = Se or Te) in tetrahydrofuran (thf) at ambient temperature for periods of between 2 and 8 d afforded the air-stable complexes [2,2-$(PR_3)_2$-*closo*-2,1-$PdEB_{10}H_{10}$] **1**–**6** [equation (1)]

$$[PdCl_2(PR_3)_2] + [7\text{-}EB_{10}H_{11}]^- \xrightarrow{thf} [(PR_3)_2PdEB_{10}H_{10}] + Cl^- + HCl \quad (1)$$

as the only significant products in yields which varied from 16 (R = Ph, E = Se) to 82% ($R_3$ = $Me_2Ph$, E = Te). Table 1 lists compounds **1**–**6**, together with yields, colours, elemental analyses and observed infrared B–H absorptions. They were also characterised using $^1H$, $^{11}B$ and $^{31}P$ NMR spectroscopies, including $[^1H\text{–}^1H]$ correlation spectroscopy (COSY) and selective $^1H\text{-}\{^{11}B\}$ decoupling experiments. The NMR behaviour was strikingly similar for all six compounds and only **1** and **4** are discussed in detail (see Table 2 and Experimental section for **2**, **3**, **5** and **6**).

The identity of both compounds **1** and **4** as *closo*-$MEB_{10}$ species was readily confirmed by multielement NMR spectroscopy. Their mutually similar NMR behaviour resembles that of the previously reported platinum analogues [2,2-$(PR_3)_2$-2,1-$PtSeB_{10}H_{10}$] ($R_3$ = $Ph_3$ **7**,[2] $Bu^n_3$, $Et_3$ **8** or $Me_2Ph$ **9**[3]) and [2,2-$(PR_3)_2$-2,1-$PtTeB_{10}H_{10}$] ($R_3$ = $Et_3$ **10**, $Bu^n_3$ or $Me_2Ph$ **11**),[3] which have been fully characterised by NMR spectroscopy

† *Supplementary data available:* see Instructions for Authors, *J. Chem. Soc., Dalton Trans.*, 1993, Issue 1, pp. xxiii–xxviii.

**Table 1** Bis(phosphine) palladaheteroborane complexes [2,2-$(PR_3)_2$-*closo*-2,1-$PdEB_{10}H_{10}$] **1–6**

| Compound | $R_3$ | E | Colour | Yield (%) | Analysis * (%) C | H | ν(B–H)/cm$^{-1}$ |
|---|---|---|---|---|---|---|---|
| **1** | $Ph_3$ | Se | Wine-red | 15.8 | 52.05 (52.20) | 4.80 (4.85) | 2562s, 2522s, 2510s |
| **2** | $MePh_2$ | Se | Red | 21.3 | 44.00 (44.35) | 5.00 (5.15) | 2597m, 2563s, 2545s, 2530s (sh), 2519vs, 2490s |
| **3** | $Me_2Ph$ | Se | Rust-red | 25.3 | 32.70 (33.15) | 5.60 (5.55) | 2560s, 2542vs, 2518vs, 2476s |
| **4** | $Ph_3$ | Te | Purple | 18.4 | 48.80 (49.30) | 4.85 (4.60) | 2543vs, 2518s, 2498s |
| **5** | $MePh_2$ | Te | Purple | 53.0 | — — | — — | 2592m, 2542s, 2524s, 2519vs, 2490s, 2473s |
| **6** | $Me_2Ph$ | Te | Purple | 81.7 | 31.45 (30.55) | 5.30 (5.10) | 2522vs, 2505vs, 2495vs, 2477s |

* Calculated values in parentheses.

**Table 2** Measured NMR parameters for [2,2-$(PPh_3)_2$-*closo*-2,1-$PdEB_{10}H_{10}$] (E = Se **1** or Te **4**) and [2-Cl-2-$(PPh_3)$-*closo*-2,1-$PdTeB_{10}H_9(PPh_3)$] **12** in $CD_2Cl_2$ solution at 294–297 K

| | | **1**[a] | | | **4**[b] | | | **12**[c] | |
|---|---|---|---|---|---|---|---|---|---|
| Assignment[d] | Intensity[d] | δ($^{11}$B)[e] | $^1J(^{11}B-^1H)$[f] | δ($^1$H)[g] | δ($^{11}$B)[e] | $^1J(^{11}B-^1H)$[f] | δ($^1$H)[g] | δ($^{11}$B)[e] | δ($^1$H)[g] |
| (12) | 1 | +20.9 | 139 | +4.08 | +23.2 | 141 | +5.74 | +18.0 | +4.96 |
| (7, 11) | 2 | +13.1 | *ca.* 131[h] | +3.94 | +16.8 | *ca.* 131[h] | +4.90 | +10.5 | *i* |
| | | | | | | | | +9.2 | +3.40 |
| (9) | 1 | +5.4 | 143 | +3.92 | +9.4 | 139 | +4.96 | +3.5 | +4.73 |
| (3, 6) | 2 | +2.2[j] | *h* | +1.46 | +3.4[j] | *h* | +1.96 | +6.0[j] | +2.79 |
| | | | | | | | | −5.0[j] | +2.01 |
| (4, 5) | 2 | −9.7[j] | *h* | +2.33 | −11.0[j] | *h* | +2.76 | *ca.* −10.7[j] | +3.18 |
| | | | | | | | | *ca.* −10.7[j] | +2.79 |
| (8, 10) | 2 | −19.7 | 143 | +1.09 | −18.4 | 148 | +1.58 | −19.6 | +1.70 |
| | | | | | | | | −21.9 | +1.47 |

[a] δ($^{31}$P) +26.8. [b] δ($^{31}$P) +25.4. [c] δ($^{31}$P) +31.2(Pd) and +11.4(B); $^1J(^{31}P-^{11}B)$ 135 Hz. [d] On the basis of relative intensities together with shielding and line-width parallels with previously reported platinum analogues (see ref. 4). [e] ±0.5 ppm to high frequency (low field) of $BF_3(OEt_2)$. [f] ±8 Hz; measured from resolution-enhanced $^{11}$B spectrum. [g] ±0.05 Hz to high frequency (low field) of $SiMe_4$; $^1$H resonances were related to directly bound B positions by $^1$H-{$^{11}$B(selective)} spectroscopy. [h] Insufficiently resolved for accurate estimation. [i] P substituent on B(7) or B(11). [j] These $^{11}$B resonance lines are substantially broader (*i.e.* 300–400 Hz) than the other lines (< *ca.* 200 Hz).



and, for **7**,[2] **8** and **10**,[3] by single-crystal X-ray diffraction. The 1:2:1:2:2:2 relative intensity patterns in the $^{11}$B NMR spectra of **1–6** are consistent with *closo*-2,1-$PdEB_{10}$ clusters having a mirror plane of symmetry. The two broader resonances (Table 2) are ascribed to the $^{11}$B(3,6) and $^{11}$B(4,5) positions since these are known to have shorter relaxation times, $T_1(^{11}B)$, associated with them in the other *closo*-2,1-$PtEB_{10}$ compounds that have been reported.[3,4] The assignments of the other $^{11}$B resonances then follow from their relative intensities and general shielding parallels with the previously reported species. The $^1$H resonances were assigned to their directly bound boron atom positions by $^1$H-{$^{11}$B(selective)} spectroscopy. No bridging $^1$H resonances were observed in any of the $^1$H NMR spectra.

The similarity among the PdSe **1**, PdTe **4**, PtSe **7** and PtTe **11** compounds is illustrated in Fig. 1 which plots δ($^{11}$B) *versus* δ($^1$H) for directly bound B–H units in the four compounds. The data for each position fall in closely defined regions. The principal differences among the compounds on changing from Pt to Pd are (*i*) a decrease in $^{11}$B nuclear shielding at the (3,6) and (7,11) positions adjacent to the metal atom and (*ii*) changes in the $^1$H nuclear shielding in the 9 position which is antipodal to the metal atom in the 2 position. For the platinum compounds this $^1$H(9) shielding is anomalously low (and is diagnostic of an antipodal position to third-row transition elements)[3–5] whereas for the two palladium compounds the data fall nearer to a line of general correlation. Similar considerations apply to the data from the 12 position, where it can be seen that the $^1$H nuclei in positions antipodal to tellurium exhibit anomalously low shielding. For all four compounds the δ($^{11}$B,$^1$H) (3,6) data fall some 1 or 2 ppm in δ($^1$H) above the general shielding correlation. A fluxional process associated with metal-to-heteroborane bonding was revealed by a variable-temperature $^1$H-{$^{31}$P} NMR study of

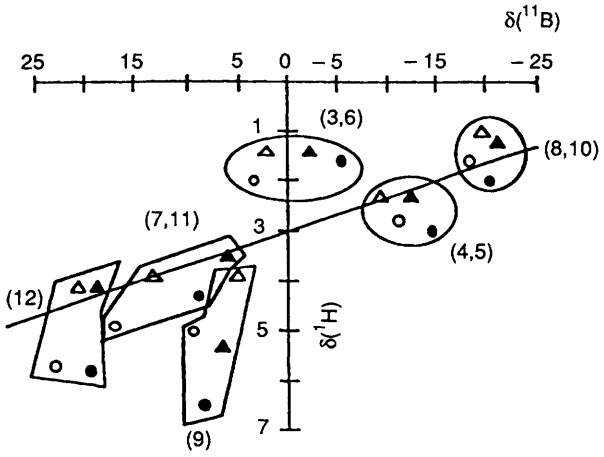


**Fig. 1** Plot of δ($^{11}$B) *versus* δ($^1$H) for the directly bound boron and hydrogen atoms of [2,2-$(PR_3)_2$-*closo*-2,1-$MEB_{10}H_{10}$] complexes where $(PR_3)_2ME$ is $(PPh_3)_2PdSe$ **1** (Δ), $(PPh_3)_2PdTe$ **4** (○), $(PPh_3)_2PtSe$ **7** (▲) and $(PMe_2Ph)_2PtTe$ **11** (●). The line drawn has slope δ($^{11}$B):δ($^1$H) of 15:1 and intercept of +3.0 in δ($^1$H)

[2,2-$(PMe_2Ph)_2$-*closo*-2,1-$PdSeB_{10}H_{10}$] **3**. The P-methyl region of the $^1$H NMR spectrum of compound **3** at 225 K consisted of two resonances centred at δ + 1.59 and + 1.37, which coalesced on heating to above 293 K into one peak at δ 1.54. This type of non-dissociative mutual rotation of the $\eta^5$-heteroborane cage and the $PdP_2$ unit about an axis passing through the metal and the BH(12) unit opposite is similar to that for the $\eta^4$-co-ordination mode in the eleven-vertex [7,7-$(PMe_2Ph)_2$-*nido*-7-$PtB_{10}H_{12}$].[6,7]

The value of $\Delta G^{\ddagger}$ for the fluxional process in **3** was 44.5 kJ mol$^{-1}$ at the coalescence temperature of 293 K. This can be

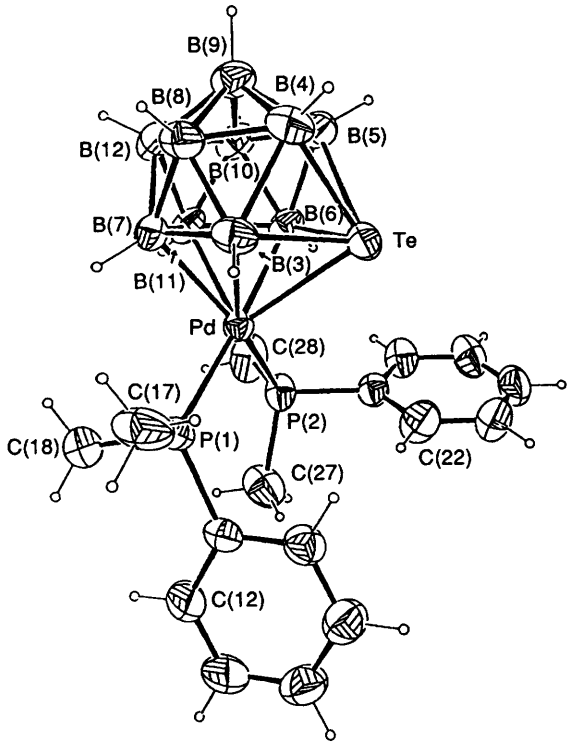


**Fig. 2** A view of [2,2-$(PMe_2Ph)_2$-*closo*-2,1-$PdTeB_{10}H_{10}$] **6** with the atom numbering scheme

compared to values of 58 and 62 kJ $mol^{-1}$ for [2,2-$(PMe_2Ph)_2$-*closo*-2,1-$PtEB_{10}H_{10}$] (E = Se or Te), respectively,[3,4] *ca.* 58 kJ $mol^{-1}$ for [1-Ph-2,2-$(PMe_2Ph)_2$-*closo*-2,1-$PtPB_{10}H_{10}$],[8] and a range of values from 35 to > 75 kJ $mol^{-1}$ reported for several isoelectronic rhodium and iridium carbaboranes of general formulae $[(PR_3)_2(H)M(C_2R_2B_9H_9)]$.[9]

The molecular structure of **6** is shown in Fig. 2 and selected interatomic distances and angles are given in Table 3. The $PdTeB_{10}$ cage contains adjacent Pd and Te atoms with a Pd–Te bond length of 2.6833(2) Å. No previous reports of structures of palladium derivatives of Group 16 heteroboranes are in the literature, but a Pd–Te distance of 2.606(1) Å was calculated in *trans*-$[Pd(SCN)_2(TeR_2)_2]$ [R = $(CH_2)_3SiMe_3$].[10]

The Pd–B distances in **6** range from 2.234(3) to 2.301(3) Å. The Te–B distances vary from 2.294(4) to 2.374(3) Å. A slightly larger range, 2.291(8)–2.404(8) Å, was observed for the related compound [2,2-$(PEt_3)_2$-*closo*-2,1-$PtTeB_{10}H_{10}$] **10**.[4] In general, the Pd–B and Te–B distances in **6** follow the same trends previously found for the platinaselena- and platinatellura-boranes[2–4] such as **10**. The Te–B(3,6) and Pd–B(3,6) bond lengths are considerably longer than the Te–B(4,5) and Pd–B (7,11) distances (see Table 3).

Large variations in B–B distances [1.733(5)–1.940(4) Å] were observed in **6** and this was also the case for **10** [1.728(12)–1.948(13) Å]. The longest B–B distances were observed for B(3)–B(4) 1.940(4), B(5)–B(6) 1.932(5) and B(4)–B(5) 1.868(5) Å, *i.e.* the B–B bonds which flank the Pd–Te linkage.

The Pd–P bond lengths are slightly but not significantly different at 2.3301(7) and 2.3354(8) Å. Comparison can be made with Pd–P distances in [3,3-$(PMe_3)_2$-*closo*-3,1,2-$PdC_2B_9H_{11}$] which were significantly shorter at 2.280(1) and 2.302(1) Å.[11]

In an attempt to extend the metal-centred chemistry of metallaheteroboranes, we synthesised [2-X-2-$(PPh_3)$-*closo*-2,1-$PdTeB_{10}H_9(PPh_3)$] (X = Cl **12** or I **13**) and studied substitution reactions at the Pd–I bond in **13**. Although $[PdX_2(PR_3)_2]$ complexes may exist as either *cis* or *trans* isomers in the solid state, they often exist as a mixture of isomers

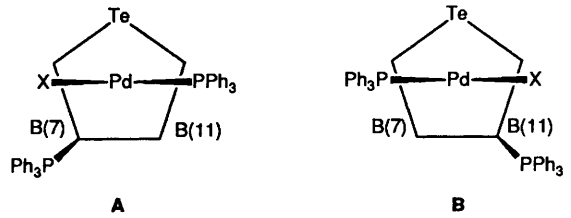


**Scheme 1**

in common organic solvents such as $CHCl_3$ or acetone.[12,13] However, there are combinations of R, X and solvent which provide solutions of $[PdX_2(PR_3)_2]$ compounds which are specifically *cis* or *trans*. By choosing R = Ph, X = Cl or I and refluxing toluene as solvent we were able to examine the reactions of *trans*-$[PdX_2(PPh_3)_2]$ with $Cs[TeB_{10}H_{11}]$ which afforded complexes **12** and **13** in 39 and 95% yields respectively [equation (2)].

$$[PdI_2(PPh_3)_2] + Cs[TeB_{10}H_{11}] \xrightarrow{\text{refluxing toluene}} \mathbf{13} + CsI + H_2 \quad (2)$$

The infrared spectra of **12** and **13** contained strong B–H absorptions at 2538 and 2552 $cm^{-1}$ respectively. At 80.4 MHz, the $^{11}B$-$\{^1H\}$ NMR spectra of **12** and **13** showed eight peaks in an intensity pattern of 1:1:1:2:1:2:1:1. In both spectra one signal of unit intensity was coupled to phosphorus with $^1J(^{11}B–^{31}P)$ = 135 Hz for **12** and 129 Hz for **13**. Both the 128 MHz $^{11}B$-$\{^1H\}$ and 400 MHz $^1H$-$\{^{11}B\}$ NMR spectra of **12** exhibited ten borane peaks which were correlated using $^1H$-$\{^1B(selective)\}$ experiments (Table 2). The assignments were based on comparisons with the data from **1** and **4**, and the recognition of the peak due to the $B(PPh_3)$ unit. The chemical shifts of the peaks in the spectra of **12** and **13** were very similar to those for **1** and **4** (Table 2) and support the proposed $PdTeB_{10}$-cage structure. However, in **12** and **13** different cage-substituted stereoisomers are possible depending on the arrangement of the $PdX(PPh_3)$ and $B(PPh_3)$ units. Scheme 1 shows the most likely cage-substituted (7-$PPh_3$ and 11-$PPh_3$) isomers **A** and **B** assuming that the steric interactions between the phosphine ligands are minimised. The formation of both isomers is equally possible and compounds **12** and **13** are presumably formed as a 1:1 mixture of these isomers.

The reaction of **13** with mercury(II) salts $HgX_2$ (X = Cl, Br, CN, SCN or $O_2CMe$) in a 1:1.1 molar ratio in thf at room temperature for 24 h afforded $[\{PdX(PPh_3)\}TeB_{10}H_9(PPh_3)]$ in yields ranging from 19 (X = $O_2CMe$, **14**) to 96% (X = CN, **15**). These compounds all contained strong B–H absorptions in the region of 2540 $cm^{-1}$ in their infrared spectra and showed very similar $^{11}B$-$\{^1H\}$ NMR spectra to those of **12** and **13** indicating that the $PdTeB_{10}$-cage structures were analogous.

The overall structure of the Pd–X-containing compounds was established for complex **14** by a single-crystal X-ray diffraction study. Suitable crystals of [2-$(O_2CMe)$-2-$(PPh_3)$-*closo*-2,1-$PdTeB_{10}H_9(PPh_3)$]·$0.79CH_2Cl_2$ were grown from a $CH_2Cl_2$–*n*-$C_7H_{14}$ solution. The molecular structure of **14**·$0.79CH_2Cl_2$ as the isomer **B**, *i.e.* with the $B(PPh_3)$ unit at site B(11) is shown in Fig. 3 and selected interatomic distances and angles are given in Table 4. It has the same $PdTeB_{10}$-cage structure and the same conformation of the PdXL unit above the $TeB_4$ face as compound **6**. The $Pd(PPh_3)$ and $B(PPh_3)$ ligands are arranged to minimise steric interactions and the acetate ligand is monodentate with Pd–O(1) 2.121(3) Å [*cf.* Pd · · · O(2) 3.189(4) Å].

The monodentate nature of the acetate ligand is unusual for palladium complexes which usually prefer the acetate group as a bidentate ligand to a single palladium or, more usually, as a bridging ligand between two palladium centres. An example of

**Table 3** Selected interatomic distances (Å) and angles (°) for [2,2-$(PMe_2Ph)_2$-*closo*-2,1-$PdTeB_{10}H_{10}$] **6**

| | | | | | | | |
|---|---|---|---|---|---|---|---|
| Pd–Te | 2.6833(2) | Te–B(6) | 2.374(3) | B(5)–B(10) | 1.769(5) | B(10)–B(11) | 1.768(4) |
| Pd–P(1) | 2.3301(7) | B(3)–B(4) | 1.940(4) | B(6)–B(10) | 1.762(4) | B(10)–B(12) | 1.761(5) |
| Pd–P(2) | 2.3354(8) | B(3)–B(7) | 1.849(5) | B(6)–B(11) | 1.831(4) | B(11)–B(12) | 1.764(5) |
| Pd–B(3) | 2.301(3) | B(3)–B(8) | 1.733(5) | B(7)–B(8) | 1.773(4) | P(1)–C(11) | 1.818(3) |
| Pd–B(6) | 2.290(3) | B(4)–B(5) | 1.868(5) | B(7)–B(11) | 1.777(5) | P(1)–C(17) | 1.810(4) |
| Pd–B(7) | 2.234(3) | B(4)–B(8) | 1.742(5) | B(7)–B(12) | 1.761(4) | P(1)–C(18) | 1.809(4) |
| Pd–B(11) | 2.259(3) | B(4)–B(9) | 1.735(5) | B(8)–B(9) | 1.774(4) | P(2)–C(21) | 1.813(3) |
| Te–B(3) | 2.345(3) | B(5)–B(6) | 1.932(5) | B(8)–B(12) | 1.767(5) | P(2)–C(27) | 1.832(3) |
| Te–B(4) | 2.294(4) | B(5)–B(9) | 1.749(5) | B(9)–B(10) | 1.786(5) | P(2)–C(28) | 1.815(4) |
| Te–B(5) | 2.301(3) | | | B(9)–B(12) | 1.756(5) | | |
| P(1)–Pd–P(2) | 98.31(3) | B(4)–B(3)–B(8) | 56.3(2) | Pd–B(7)–B(3) | 67.8(1) | B(9)–B(10)–B(12) | 59.4(2) |
| Te–Pd–P(1) | 124.52(3) | B(7)–B(3)–B(8) | 59.2(2) | Pd–B(7)–B(11) | 67.4(2) | B(11)–B(10)–B(12) | 60.0(2) |
| Te–Pd–P(2) | 105.79(2) | Te–B(4)–B(3) | 66.7(1) | B(3)–B(7)–B(8) | 57.1(2) | Pd–B(11)–B(6) | 67.2(1) |
| Te–Pd–B(3) | 55.50(8) | Te–B(4)–B(5) | 66.2(2) | B(8)–B(7)–B(12) | 60.0(2) | Pd–B(11)–B(7) | 66.0(1) |
| Te–Pd–B(6) | 56.35(8) | B(3)–B(4)–B(8) | 55.8(2) | B(11)–B(7)–B(12) | 59.8(2) | B(6)–B(11)–B(10) | 58.6(2) |
| B(3)–Pd–B(6) | 84.4(1) | B(5)–B(4)–B(9) | 57.9(2) | B(3)–B(8)–B(4) | 67.9(2) | B(7)–B(11)–B(12) | 59.7(2) |
| B(3)–Pd–B(7) | 48.1(1) | B(8)–B(4)–B(9) | 61.4(2) | B(3)–B(8)–B(7) | 63.6(2) | B(10)–B(11)–B(12) | 59.8(2) |
| B(6)–Pd–B(11) | 47.5(1) | Te–B(5)–B(4) | 65.8(2) | B(4)–B(8)–B(9) | 59.1(2) | B(7)–B(12)–B(8) | 60.3(2) |
| B(7)–Pd–B(11) | 46.6(1) | Te–B(5)–B(6) | 67.6(1) | B(7)–B(8)–B(12) | 59.7(2) | B(7)–B(12)–B(11) | 60.6(2) |
| Pd–Te–B(3) | 53.95(7) | B(4)–B(5)–B(9) | 57.2(2) | B(9)–B(8)–B(12) | 59.5(2) | B(8)–B(12)–B(9) | 60.5(2) |
| Pd–Te–B(6) | 53.43(7) | B(6)–B(5)–B(10) | 56.7(2) | B(4)–B(9)–B(5) | 64.8(2) | B(9)–B(12)–B(10) | 61.0(2) |
| B(3)–Te–B(4) | 49.4(1) | B(9)–B(5)–B(10) | 61.0(2) | B(4)–B(9)–B(8) | 59.5(2) | B(10)–B(12)–B(11) | 60.2(2) |
| B(4)–Te–B(5) | 48.0(1) | Te–B(6)–Pd | 70.22(9) | B(5)–B(9)–B(10) | 60.0(2) | Pd–P(1)–C(18) | 108.9(1) |
| B(5)–Te–B(6) | 48.8(1) | Te–B(6)–B(5) | 63.6(1) | B(8)–B(9)–B(12) | 60.1(2) | Pd–P(2)–C(21) | 110.89(9) |
| B(3)–Te–B(6) | 81.6(1) | Pd–B(6)–B(11) | 65.4(1) | B(10)–B(9)–B(12) | 59.6(2) | Pd–P(2)–C(27) | 121.8(1) |
| Te–B(3)–Pd | 70.6(1) | B(5)–B(6)–B(10) | 57.0(2) | B(5)–B(10)–B(6) | 66.3(2) | Pd–P(2)–C(28) | 113.8(1) |
| Te–B(3)–B(4) | 63.9(2) | B(10)–B(6)–B(11) | 58.9(2) | B(5)–B(10)–B(9) | 59.0(2) | Pd–P(1)–C(11) | 118.95(9) |
| Pd–B(3)–B(7) | 64.1(1) | | | B(6)–B(10)–B(11) | 62.5(2) | Pd–P(1)–C(17) | 118.53(9) |

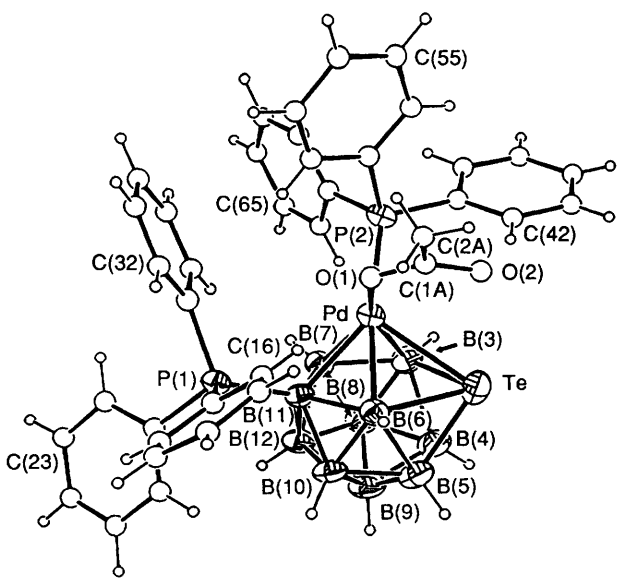


**Fig. 3** A view of [2-$(O_2CMe)$-2,11-$(PPh_3)_2$-*closo*-2,1-$PdTeB_{10}H_9$]·0.79$CH_2Cl_2$ **14**·0.79$CH_2Cl_2$ with the atom numbering scheme

the monodentate mode is found in the complex (acetato){2-ethoxy-1-ethoxycarbonyl-1-[6-(3-ethoxy-2-ethoxycarbonyl-3-oxopropyl)-2,2′-bipyridin-6′-ylmethyl]-2-oxoethyl-*C*,*N*,*N*′}-palladium **16**.[14] The compounds described in refs. 15–18 contain acetate in the bridging mode, a typical example being di-μ-acetato-*O*,*O*′-bis[(8-methoxynaphthyl-$C^1$,*O*)palladium(II)] **17**.[18] The Pd–O distance in **14** is significantly longer than the distance in **16**, 2.047 Å,[14] but is within the wide range of values found in the bridged systems reported in refs. 15–18, *i.e.* 2.03(1)[17]–2.198(7) Å.[15] The angles Pd–O–C 118.6(3) and O–C–O 126.4(4)° in **14** are typical for the acetate ligand irrespective of the bonding mode.[14–18]

The Pd–Te distance in **14**, 2.6903(4) Å, is longer than in **6** and the palladium atom is bonded to B(3,6,7,11) in a more asymmetrical fashion in **14** compared to **6** with the Pd–B(7) and Pd–B(11) distances significantly different at 2.201(5) and 2.252(4) Å respectively. The ranges for the Te–B and B–B distances in **14** are 2.286(6)–2.401(4) and 1.753(7)–1.978(7) Å respectively, which are similar to those in **6**. The Pd–P distance in **14**, 2.355(1) Å, is longer than either of the Pd–P distances in **6** (Table 3). The B(11)–P distance, 1.942(4) Å, is longer than the range of reported B–P distances of 1.87–1.93 Å.[19]

Some comments on the syntheses of [2-X-2-$(PPh_3)$-*closo*-2,1-$PdTeB_{10}H_9(PPh_3)$] compounds are pertinent. As far as a strategy for the synthesis of [2-Cl-2-$(PPh_3)$-*closo*-2,1-$PdTeB_{10}H_9(PPh_3)$] **12** is concerned, it is clear that the chloride substitution reaction using the PdI compound **13** is far superior to the direct reaction between $[TeB_{10}H_{11}]^-$ and $[PdCl_2(PPh_3)_2]$ in toluene. The yield of **12** from the former reaction is about twice that from the latter. It is also noteworthy that excellent yields of the corresponding PdBr **18** and PdCN **15** compounds were obtained from substitution reactions. However, disappointingly low yields of the palladium nitrogen-bound thiocyanate **19** and the acetate **14** compounds were obtained.

## Experimental

*General.*—All preparative experiments and recrystallisations were carried out in an inert atmosphere. The compounds $[PdCl_2(PPh_3)_2]$,[20] $[PdCl_2(PMe_2Ph)_2]$,[21] $[PdI_2(PPh_3)_2]$,[13] $Cs[SeB_{10}H_{11}]$ and $Cs[TeB_{10}H_{11}]$[22] were prepared according to literature methods while $[PdCl_2(PMePh_2)_2]$ was prepared using the same method as for $[PdCl_2(PMe_2Ph)_2]$.[21] Infrared spectra were recorded as KBr discs on a Perkin Elmer 682 or a Mattson Polaris FTIR spectrometer. NMR spectroscopy was carried out as described in earlier parts of this series,[1–5] with chemical shifts (δ) quoted in ppm to low frequency (high field) of Ξ 100 MHz for $^1H$, Ξ 40.480 730 MHz for $^{31}P$ (nominally 85% $H_3PO_4$) and Ξ 32.083 971 MHz for $^{11}B$ [nominally $BF_3(OEt_2)$ in $CD_2Cl_2$]; the complex coupling constant $N = {}^2J + {}^4J$.

*Synthesis of Compounds* [2,2-$(PR_3)_2$-*closo*-2,1-$PdEB_{10}H_{10}$] **1**–**6** ($R_3$ = $Ph_3$, $Me_2Ph$ *or* $MePh_2$; E = Se *or* Te).—*General procedure.* Reactions were carried out on a 0.5 mmol scale

**Table 4** Selected interatomic distances (Å) and angles (°) for [2-($O_2$CMe)-2-($PPh_3$)-*closo*-2,1-$PdTeB_{10}H_9(PPh_3)$]·0.79$CH_2Cl_2$ **14**·0.79$CH_2Cl_2$

| | | | | | | | |
|---|---|---|---|---|---|---|---|
| Pd–Te | 2.6903(4) | B(3)–B(4) | 1.978(7) | B(6)–B(11) | 1.833(5) | O(1)–C(1A) | 1.232(4) |
| Pd–P(2) | 2.355(1) | B(3)–B(7) | 1.888(5) | B(7)–B(8) | 1.806(7) | O(2)–C(1A) | 1.251(5) |
| Pd–O(1) | 2.121(3) | B(3)–B(8) | 1.790(7) | B(7)–B(11) | 1.778(6) | C(1A)–C(2A) | 1.515(8) |
| Pd–B(3) | 2.243(6) | B(4)–B(5) | 1.868(8) | B(7)–B(12) | 1.781(6) | P(1)–C(11) | 1.804(4) |
| Pd–B(6) | 2.268(4) | B(4)–B(8) | 1.799(6) | B(8)–B(9) | 1.809(6) | P(1)–C(21) | 1.813(4) |
| Pd–B(7) | 2.201(5) | B(4)–B(9) | 1.753(7) | B(8)–B(12) | 1.783(6) | P(1)–C(31) | 1.806(4) |
| Pd–B(11) | 2.252(4) | B(5)–B(6) | 1.926(8) | B(9)–B(10) | 1.795(8) | P(1)–B(11) | 1.942(4) |
| Te–B(3) | 2.384(4) | B(5)–B(9) | 1.764(8) | B(9)–B(12) | 1.780(6) | P(2)–C(41) | 1.820(4) |
| Te–B(4) | 2.289(6) | B(5)–B(10) | 1.798(6) | B(10)–B(11) | 1.786(6) | P(2)–C(51) | 1.824(5) |
| Te–B(5) | 2.286(6) | B(6)–B(10) | 1.793(8) | B(10)–B(12) | 1.782(6) | P(2)–C(61) | 1.825(3) |
| Te–B(6) | 2.401(4) | | | B(11)–B(12) | 1.765(7) | | |
| P(2)–Pd–O(1) | 90.7(1) | Pd–B(3)–B(7) | 63.7(2) | Pd–B(7)–B(3) | 66.0(2) | Pd–B(11)–B(6) | 66.5(2) |
| Te–Pd–O(1) | 102.80(6) | B(4)–B(3)–B(8) | 56.8(3) | Pd–B(7)–B(11) | 68.0(2) | Pd–B(11)–B(7) | 65.0(2) |
| Te–Pd–P(2) | 116.78(2) | B(7)–B(3)–B(8) | 58.7(3) | B(3)–B(7)–B(8) | 57.9(3) | B(6)–B(11)–B(10) | 59.4(3) |
| Te–Pd–B(3) | 56.9(1) | Te–B(4)–B(3) | 67.5(2) | B(8)–B(7)–B(12) | 59.6(3) | B(7)–B(11)–B(12) | 60.3(3) |
| Te–Pd–B(6) | 57.2(1) | Te–B(4)–B(5) | 65.8(3) | B(11)–B(7)–B(12) | 59.5(3) | B(10)–B(11)–B(12) | 60.2(3) |
| B(3)–Pd–B(6) | 86.9(2) | B(3)–B(4)–B(8) | 56.4(2) | B(3)–B(8)–B(4) | 66.9(3) | B(7)–B(12)–B(8) | 60.9(3) |
| B(3)–Pd–B(7) | 50.3(2) | B(5)–B(4)–B(9) | 57.9(2) | B(3)–B(8)–B(7) | 63.3(3) | B(7)–B(12)–B(11) | 60.2(3) |
| B(3)–Pd–B(11) | 84.6(2) | B(8)–B(4)–B(9) | 61.2(3) | B(4)–B(8)–B(9) | 58.1(3) | B(8)–B(12)–B(9) | 61.0(3) |
| B(6)–Pd–B(7) | 83.2(2) | Te–B(5)–B(4) | 66.0(3) | B(7)–B(8)–B(12) | 59.5(3) | B(9)–B(12)–B(10) | 60.5(3) |
| B(6)–Pd–B(11) | 47.8(1) | Te–B(5)–B(6) | 67.6(1) | B(9)–B(8)–B(12) | 59.4(2) | B(10)–B(12)–B(11) | 60.5(3) |
| B(7)–Pd–B(11) | 47.0(2) | B(4)–B(5)–B(9) | 57.2(2) | B(4)–B(9)–B(5) | 64.2(3) | Pd–P(2)–C(41) | 115.4(1) |
| Pd–Te–B(3) | 52.0(1) | B(6)–B(5)–B(10) | 57.4(3) | B(4)–B(9)–B(8) | 60.6(3) | Pd–P(2)–C(51) | 110.2(1) |
| Pd–Te–B(6) | 52.5(1) | B(9)–B(5)–B(10) | 60.5(3) | B(5)–B(9)–B(10) | 60.7(3) | Pd–P(2)–C(61) | 120.7(1) |
| B(3)–Te–B(4) | 50.0(2) | Te–B(6)–Pd | 70.3(1) | B(8)–B(9)–B(12) | 59.6(2) | Pd–O(1)–O(2) | 91.6(2) |
| B(4)–Te–B(5) | 48.2(2) | Te–B(6)–B(5) | 62.7(2) | B(10)–B(9)–B(12) | 59.8(3) | Pd–O(1)–C(1A) | 118.6(3) |
| B(5)–Te–B(6) | 48.5(2) | Pd–B(6)–B(11) | 65.6(2) | B(5)–B(10)–B(6) | 64.9(3) | Pd–O(1)–C(2A) | 154.1(2) |
| B(3)–Te–B(6) | 80.9(2) | B(5)–B(6)–B(10) | 57.7(3) | B(6)–B(10)–B(11) | 61.6(3) | O(1)–C(1A)–O(2) | 126.4(4) |
| Te–B(3)–Pd | 71.1(1) | B(10)–B(6)–B(11) | 59.0(2) | B(9)–B(10)–B(12) | 59.7(3) | O(1)–C(1A)–C(2A) | 116.2(4) |
| Te–B(3)–B(4) | 62.5(2) | | | B(11)–B(10)–B(12) | 59.3(3) | O(2)–C(1A)–C(2A) | 117.4(4) |



with equimolar amounts of reagents. To a solution of Cs[7-$EB_{10}H_{11}$] (E = Se or Te) in thf (30 $cm^3$) was added [$PdCl_2(PR_3)_2$] ($R_3$ = $Ph_3$, $Me_2Ph$ or $MePh_2$) as a solution or suspension in thf (30 $cm^3$). The reation mixture was stirred at room temperature for *ca.* 2–8 d (*i.e.* until the reaction was complete; monitored by TLC). The solution was filtered, concentrated under reduced pressure at 25 °C and subjected to preparative TLC ($CH_2Cl_2$–hexane, 4:1 or 3:2 as eluent). The single major band was extracted into $CH_2Cl_2$ and purified by repeated chromatography (100% $CH_2Cl_2$ or $CH_2Cl_2$–hexane, 4:1). Recrystallisation from $CH_2Cl_2$ or ($CH_2Cl_2$–cyclohexane, 3:1) afforded **1**–**6** in low to high yields, Table 1. Elemental analyses (C, H) and selected infrared data are given in Table 1.

*Reaction of* [7-$SeB_{10}H_{11}$]$^-$ *and* [$PdCl_2(PPh_3)_2$]. The product was recrystallised from $CH_2Cl_2$–cyclohexane (3:1) to give red platelets of [2,2-$(PPh_3)_2$-*closo*-2,1-$PdSeB_{10}H_{10}$] **1**. Table 2 lists $^1$H, $^{11}$B and $^{31}$P NMR data.

*Reaction of* [7-$SeB_{10}H_{11}$]$^-$ *and* [$PdCl_2(PPh_2Me)_2$]. The product was recrystallised from $CH_2Cl_2$ affording microcrystalline red needles of [2,2-$(PPh_2Me)_2$-*closo*-2,1-$PdSeB_{10}H_{10}$] **2**. NMR ($CD_2Cl_2$, 294–297 K) ordered as (assignment) δ($^{11}$B) [δ($^1$H) of directly bound $^1$H atom in square brackets]: (12) +21.1 [+4.17], (7,11) +12.5 [+3.87], (9) +4.5 [+3.98], (3,6) −0.1 (br) [+1.23], (4,5) −9.6 (br) [+2.49] and (8,10) −20.3 [+1.17]; δ($^1$H) +1.82 (Me); $N$($^{31}$P–$^1$H) 8.7 Hz; δ($^{31}$P) +9.5.

*Reaction of* [7-$SeB_{10}H_{11}$]$^-$ *and* [$PdCl_2(PMe_2Ph)_2$]. Recrystallisation from $CH_2Cl_2$ afforded rust-red crystals of [2,2-$(PMe_2Ph)_2$-*closo*-2,1-$PdSeB_{10}H_{10}$] **3**. NMR ($CD_2Cl_2$, 294–297 K): (12) +20.6 [$^1J$($^{11}$B–$^1$H) 139] [+4.18], (7,11) +11.3 [$^1J$($^{11}$B–$^1$H) 136] [+3.69], (9) +3.8 [$^1J$($^{11}$B–$^1$H) 144] [+4.04], (3,6) −1.6 (br) [$^1J$($^{11}$B–$^1$H) *ca.* 147] [+1.52], (4,5) −9.9 (br) [$^1J$($^{11}$B–$^1$H) *ca.* 150] [+2.58] and (8,10) −20.5 [$^1J$($^{11}$B–$^1$H) 153 Hz] [+1.29]; (233 K) δ($^1$H) +1.59 and +1.37 (Me) (at 293 K coalescence occurs to give one resonance position at +1.54, $\Delta G^{\ddagger}$ = 44.5 kJ $mol^{-1}$), +7.4 to +7.5 (aryl); δ($^{31}$P) −5.1.

*Reaction of* [7-$TeB_{10}H_{11}$]$^-$ *and* [$PdCl_2(PPh_3)_2$]. Recrystallisation from $CH_2Cl_2$ gave purple crystals of [2,2-$(PPh_3)_2$-*closo*-2,1-$PdTeB_{10}H_{10}$] **4**. NMR data are given in Table 2.

*Reaction of* [7-$TeB_{10}H_{11}$]$^-$ *and* [$PdCl_2(PPh_2Me)_2$]. Recrystallisation from $CH_2Cl_2$ gave [2,2-$(PPh_2Me)_2$-*closo*-2,1-$PdTeB_{10}H_{10}$] **5** as purple microcrystals. NMR ($CD_2Cl_2$, 294–297 K): (12) +23.6 [+5.86], (7,11) +16.9 [+4.74], (9) +8.8 [+5.03], (3,6) +1.0 (br) [+1.66], (4,5) −10.5 (br) [+2.94] and (8,10) −19.0 [+1.57]; δ($^1$H) +1.85 (Me); $N$($^{31}$P–$^1$H) 8.6 Hz; δ($^{31}$P) +8.4.

*Reaction of* [7-$TeB_{10}H_{11}$]$^-$ *and* [$PdCl_2(PMe_2Ph)_2$]. Recrystallisation from $CH_2Cl_2$–cyclohexane (3:1) afforded purple crystals of [2,2-$(PMe_2Ph)_2$-*closo*-2,1-$PdTeB_{10}H_{10}$] **6**. NMR ($CD_2Cl_2$, 294–297 K): (12) +23.2 [+5.87], (7,11) +16.0 [+4.57], (9) +8.2 [+5.12], (3,6) −0.6 (br) [+1.93], (4,5) −10.7 (br) [+3.07] and (8,10) −19.2 [+1.66]; δ($^1$H) +1.54 (Me) (br s, suggesting coalescence just below ambient temperature, $\Delta G^{\ddagger}$ *ca.* 42 kJ $mol^{-1}$), +7.3 to +7.6 (aryl); δ($^{31}$P) −5.2.

*Reaction of* [7-$TeB_{10}H_{11}$]$^-$ *and* [$PdCl_2(PPh_3)_2$] *in Toluene*.—To a suspension of Cs[$TeB_{10}H_{11}$] (0.060 g, 0.158 mmol) in toluene (30 $cm^3$) was added a suspension of [$PdCl_2(PPh_3)_2$] (0.111 g, 0.158 mmol) in toluene (20 $cm^3$). The reaction mixture was refluxed for 17 h, then cooled and filtered. The toluene was removed under reduced pressure. The mixture was dissolved in $CH_2Cl_2$ and subjected to preparative TLC [silica gel, $CH_2Cl_2$–heptane (7:3) as eluent]. The major component was extracted into $CH_2Cl_2$. Recrystallisation from $CH_2Cl_2$–heptane (3:1) gave green crystals of [2-Cl-2-$(PPh_3)$-*closo*-2,1-$PdTeB_{10}H_9(PPh_3)$] **12** (0.055 g, 38.5%) (Found: C, 47.40; H, 4.50. $C_{36}H_{39}B_{10}ClP_2PdTe$ requires C, 47.45; H, 4.30%). IR: $\nu_{max}$(B–H) 2538 $cm^{-1}$. NMR data are given in Table 2.

*Reaction of* $[7\text{-}TeB_{10}H_{11}]^-$ *and* $[PdI_2(PPh_3)_2]$ *in Toluene.*—To a suspension of $Cs[TeB_{10}H_{11}]$ (0.225 g, 0.593 mmol) in toluene (150 $cm^3$) was added a suspension of $[PdI_2(PPh_3)_2]$ (0.525 g, 0.593 mmol) in toluene (50 $cm^3$). The reaction mixture was refluxed for 17 h, then cooled and filtered, and the toluene was removed under reduced pressure. The product was recrystallised from $CH_2Cl_2$–heptane (3:2) affording dark green crystals of [2-I-2-($PPh_3$)-*closo*-2,1-$PdTeB_{10}H_9(PPh_3)$] **13** (0.5678 g, 95.4%) (Found: C, 43.95; H, 3.80. $C_{36}H_{39}B_{10}IP_2PdTe$ requires C, 43.15; H, 3.90%). IR: $\nu_{max}$(B–H) 2552 $cm^{-1}$. NMR: $^{11}B\text{-}\{^1H\}$ ($CH_2Cl_2$, 298 K), δ + 15.6 (s, 1 B), +11.2 (s, 1 B), +10.6 [d, 1 B, $J(^{11}B\text{–}^{31}P)$ *ca.* 135 ± 5 Hz], +4.0 (s, 2 B), − 10.1 (s, 3 B), −18.5 (s, 1 B) and − 21.3 (s, 1 B); $^{31}P$ ($CD_2Cl_2$), δ 27.0 (s, 1 P) and 7.2 (q, 1 P).

*Synthesis of Compounds* [2-X-2-($PPh_3$)-*closo*-2,1-$PdTeB_{10}H_9(PPh_3)$] **12**, **14**, **15**, **18** *and* **19**.—*General procedure.* A solution of $HgX_2$ (0.164 mmol) in thf was added to a solution of **13** (*ca.* 0.149 g, 0.15 mmol) in thf (30 $cm^3$) resulting in an immediate colour change. The reaction mixture was stirred at room temperature for 24 h. It was concentrated under reduced pressure and subjected to preparative TLC [silica gel, $CH_2Cl_2$–heptane (7:3)]. The single major band was extracted into $CH_2Cl_2$ and recrystallised from $CH_2Cl_2$–heptane (3:1) affording **12**, **14**, **15**, **18** and **19** as crystalline solids.

*Reaction of* **13** *and* $HgCl_2$. Recrystallisation of the product from $CH_2Cl_2$–heptane (3:1) gave green crystals of [2-Cl-2-($PPh_3$)-*closo*-2,1-$PdTeB_{10}H_9(PPh_3)$] **12** (82.0%) (Found: C, 47.50; H, 4.70. $C_{36}H_{39}B_{10}ClP_2PdTe$ requires C, 47.45; H, 4.30%). IR: $\nu_{max}$ (B–H) 2538vs $cm^{-1}$. NMR data are given in Table 2.

*Reaction of* **13** *and* $HgBr_2$. Recrystallisation from $CH_2Cl_2$–heptane (3:1) gave green crystals of [2-Br-2-($PPh_3$)-*closo*-2,1-$PdTeB_{10}H_9(PPh_3)$] **18** (85.4%) (Found: C, 45.55; H, 4.25. $C_{36}H_{39}B_{10}BrP_2PdTe$ requires C, 45.25; H, 4.10%). IR: $\nu_{max}$ (B–H) 2538vs $cm^{-1}$. NMR ($CH_2Cl_2$, 298 K): $^{11}B\text{-}\{^1H\}$, δ +18.2 (s, 1 B), +11.2 (s, 1 B), +10.5 [d, 1 B, $J(^{11}B\text{–}^{31}P)$ *ca.* 135 ± 5 Hz], +5.2 (s, 2 B), −4.5 (s, 1 B), −10.0 (s, 2 B), −18.9 (s, 1 B) and −21.2 (s, 1 B).

*Reaction of* **13** *and* $Hg(CN)_2$. Recrystallisation from $CH_2Cl_2$–heptane (3:1) gave pink crystals of [2-(CN)-2-($PPh_3$)-*closo*-2,1-$PdTeB_{10}H_9(PPh_3)$] **15** (96.4%) (Found: C, 49.20; H, 4.45; N, 2.25. $C_{37}H_{39}B_{10}NP_2PdTe$ requires C, 49.30; H, 4.35; N, 1.55%). IR: $\nu_{max}$ 2540vs (B–H) and 2118 (CN) $cm^{-1}$. NMR ($CH_2Cl_2$, 298 K): $^{11}B\text{-}\{^1H\}$, δ +17.8 (s, 1 B), +8.6 (s, 1 B), +7.9 [d, 1 B, $J(^{11}B\text{–}^{31}P)$ *ca.* 140 ± 5 Hz], +3.7 (s, 2 B), −8.8 (s, 1 B), −11.0 (s, 2 B), −19.0 (s, 1 B) and −20.3 (s, 1 B).

*Reaction of* **13** *and* $Hg(SCN)_2$. Recrystallisation from $CH_2Cl_2$–heptane (3:1) gave green crystals of [2-(SCN)-2-($PPh_3$)-*closo*-2,1-$PdTeB_{10}H_9(PPh_3)$]·$CH_2Cl_2$ **19** (38.9%) (Found: C, 45.35; H, 4.15; N, 1.35. $C_{37}H_{39}B_{10}NP_2PdSTe$ requires C, 44.80; H, 4.05; N, 1.35%). IR: $\nu_{max}$ 2540vs (B–H) and 2084vs (SCN) $cm^{-1}$. NMR ($CH_2Cl_2$, 298 K): $^{11}B\text{-}\{^1H\}$, δ +19.4 (s, 1 B), +11.2 [d, 1 B, $J(^{11}B\text{–}^{31}P)$ *ca.* 135 ± 5 Hz], +10.5 (s, 1 B), +5.4 (s, 2 B), −4.8 (s, 1 B), −9.7 (s, 2 B), −16.5 (s, 1 B) and −20.2 (s, 1 B).

*Reaction of* **13** *and* $Hg(O_2CMe)_2$. Recrystallisation from $CH_2Cl_2$–heptane (3:1) gave dark blue crystals of [2-($O_2CMe$)-2-($PPh_3$)-*closo*-2,1-$PdTeB_{10}H_9(PPh_3)$]·0.79$CH_2Cl_2$ **14**·0.79$CH_2Cl_2$ (18.6%) (Found: C, 46.30; H, 4.60. $C_{38}H_{42}B_{10}O_2P_2PdTe$ requires 46.50; H, 4.40%). IR: $\nu_{max}$ 2532vs (B–H), 1555s, 1356s, 1314s ($O_2CMe$) $cm^{-1}$. NMR ($CH_2Cl_2$, 298 K): $^{11}B\text{-}\{^1H\}$, δ +15.8 (s, 1 B), +9.0 [d, 1 B, $J(^{11}B\text{–}^{31}P)$ *ca.* 135 ± 5 Hz], +8.1 (s, 1 B), +2.8 (s, 2 B), −5.8 (s, 1 B), −11.3 (s, 2 B), −20.6 (s, 1 B) and −21.9 (s, 1 B).

*Structure Determinations of* **6** *and* **14**·0.79$CH_2Cl_2$.—*Crystal data for* [2,2-($PMe_2Ph$)$_2$-*closo*-2,1-$PdTeB_{10}H_{10}$] **6**. $C_{16}H_{32}B_{10}P_2PdTe$, $M$ = 628.49, monoclinic, space group $P2_1/n$, $a$ = 13.110(3), $b$ = 10.498(3), $c$ = 19.561(3) Å, β = 105.44(1)°, $U$ = 2595(2) $Å^3$, $Z$ = 4, $D_c$ = 1.61 g $cm^{-3}$, $F$(000) = 1224, λ(Mo-Kα) = 0.710 73 Å, μ = 19.4 $cm^{-1}$, space group determined uniquely from systematic absences $h0l$ absent if $h + l = 2n + 1$ and $0k0$ absent if $k = 2n + 1$, $R$ = 0.023, $R'$ = 0.038 and goodness of fit = 1.45 for 4579 observed reflections.

*Crystal data for* [2-($O_2CMe$)-2-($PPh_3$)-*closo*-2,1-$PdTeB_{10}H_9(PPh_3)$]·0.79$CH_2Cl_2$ **14**·0.79$CH_2Cl_2$. $C_{38.79}H_{43.58}B_{10}O_2Cl_{1.58}P_2PdTe$, $M$ = 1001.9, triclinic, space group $P\bar{1}$, $a$ = 10.416(2), $b$ = 12.409(2), $c$ = 18.720(4) Å, α = 75.59(2), β = 84.10(2), γ = 70.98(1)°, $U$ = 2215(1) $Å^3$, $Z$ = 2, $D_c$ = 1.50 g $cm^{-3}$, $F$(000) = 994, λ(Mo-Kα) = 0.710 73 Å, μ = 12.6 $cm^{-1}$, space group determined by cell reduction and successful refinement, $R$ = 0.035, $R'$ = 0.052 and goodness of fit = 1.76 for 6472 observed reflections.

Both compounds were treated in a similar way and details of data collection and structure determination are summarised in Table 5. Accurate cell dimensions and crystal orientation matrices were determined by a least-squares refinement of the setting angles of 25 reflections. Data were collected on a CAD4 diffractometer using graphite monochromated (Mo-Kα) radiation. The intensities of three reflections measured every 2 h showed a loss in intensity for **14**·0.79$CH_2Cl_2$, so that an anisotropic decay correction was applied, with the

**Table 5** Details of data collection and refinement for **6** and **14**·0.79$CH_2Cl_2$

| | **6** | **14**·0.79$CH_2Cl_2$ |
|---|---|---|
| Crystal size/mm | 0.82 × 0.32 × 0.57 | 0.38 × 0.42 × 0.38 |
| Crystal colour and shape | Dark red block | Dark blue prism |
| Range of orienting reflections/° | 15 < θ < 20 | 9 < θ < 20 |
| Range of *hkl* collected | 0–16, 0–13, −25 to 25 | −12 to 12, −14 to 14, 0–22 |
| Scan type | ω–2θ | ω–2θ |
| Scan width | 0.6 + 0.35 tanθ | 0.9 + 0.35 tanθ |
| 2θ limits/° | 2–54 | 2–54 |
| Reflections collected | 6055 | 7793 |
| Independent reflections | 5652 | 7793 |
| Observed reflections [$I > 3\sigma(I)$] | 4579 | 6472 |
| Maximum, minimum transmission factors | 0.57, 0.41 | 1.14, 0.80 |
| Least-squares parameters | 272 | 514 |
| $R$ | 0.023 | 0.035 |
| $R'$ | 0.038 | 0.052 |
| $g$ {$[w = \sigma^2(F_o) + g(F_o^2)]^{-1}$} | 0.04 [23] | 0.0008 [24] |
| Maximum shift/error | < 0.01 | < 0.01 |
| Maximum ρ/e $Å^{-3}$ | 0.70 | 1.11 |

correction factors ranging from 0.92 to 1.06 with an average value of 1.01. No decay correction was required for **6**. Lorentz, polarisation and absorption corrections[23,25] were applied to both data sets. Both structures were solved using the Patterson heavy-atom method which revealed the positions of the Te and Pd atoms. The remaining non-hydrogen atoms were located in Fourier-difference syntheses. Hydrogen atoms (visible in difference maps) were included in the refinement at geometrically idealised positions, but restrained to ride on the carbon or boron atom to which they were bonded (C–H 0.95 or B–H 1.08 Å). Refinement was by full-matrix least-squares calculations on $F$, initially with isotropic and later with anisotropic thermal parameters for non-hydrogen atoms. There was $CH_2Cl_2$ solvent of crystallisation present in the lattice of **14** which refined to an occupancy of 0.79. In the final difference maps for both molecules **6** and **14** there were no chemically significant features.

Scattering factors and anomalous-dispersion corrections were taken from ref. 26. All calculations were performed on a PDP-11/74 computer using SDP-PLUS[23] for compound **6** and in conjunction with an IBM 3081-K mainframe computer using SHELX 76[24] for **14**·0.79$CH_2Cl_2$. Selected bond lengths and angles are given in Tables 3 and 4. Atomic coordinates are given in Tables 6 and 7. Figs. 2 and 3 are views of the molecules **6** and **14** prepared using ORTEP II[27] in conjunction with the NRCVAX suite of programs.[28]

Additional material available from the Cambridge Crystallographic Data Centre comprises H-atom coordinates, thermal parameters and remaining bond lengths and angles.

**Table 6** Positional parameters and their estimated standard deviations for [2,2-$(PMe_2Ph)_2$-*closo*-2,1-$PdTeB_{10}H_{10}$] **6**

| Atom | $x$ | $y$ | $z$ |
|---|---|---|---|
| Te | 0.208 22(2) | 0.074 35(2) | 0.335 81(1) |
| Pd | 0.042 53(1) | −0.074 26(2) | 0.274 63(1) |
| P(1) | −0.023 57(5) | −0.102 43(7) | 0.152 67(4) |
| P(2) | −0.105 16(5) | 0.024 52(7) | 0.296 65(4) |
| C(11) | −0.104 5(2) | 0.022 4(3) | 0.100 7(1) |
| C(12) | −0.202 6(2) | 0.000 3(3) | 0.055 4(2) |
| C(13) | −0.261 6(3) | 0.099 3(4) | 0.019 0(2) |
| C(14) | −0.224 5(3) | 0.221 1(3) | 0.027 7(2) |
| C(15) | −0.125 2(3) | 0.245 0(3) | 0.071 0(2) |
| C(16) | −0.065 7(2) | 0.145 9(3) | 0.107 6(2) |
| C(17) | 0.069 0(3) | −0.131 7(4) | 0.100 4(2) |
| C(18) | −0.105 8(3) | −0.243 5(3) | 0.136 6(2) |
| C(21) | −0.072 7(2) | 0.183 6(3) | 0.331 9(1) |
| C(22) | −0.038 4(3) | 0.272 9(3) | 0.290 9(2) |
| C(23) | −0.010 5(3) | 0.394 1(3) | 0.316 1(2) |
| C(24) | −0.017 0(3) | 0.426 6(3) | 0.382 4(2) |
| C(25) | −0.049 2(3) | 0.340 4(3) | 0.424 0(2) |
| C(26) | −0.076 7(2) | 0.219 3(3) | 0.399 4(2) |
| C(27) | −0.225 8(2) | 0.054 3(4) | 0.225 7(2) |
| C(28) | −0.159 0(3) | −0.059 5(3) | 0.360 3(2) |
| B(3) | 0.213 6(2) | −0.111 2(4) | 0.270 1(2) |
| B(4) | 0.327 6(3) | −0.090 3(4) | 0.355 9(2) |
| B(5) | 0.267 7(3) | −0.060 2(3) | 0.431 0(2) |
| B(6) | 0.115 6(3) | −0.063 3(3) | 0.394 6(2) |
| B(7) | 0.139 7(2) | −0.251 9(3) | 0.287 8(2) |
| B(8) | 0.279 0(2) | −0.237 2(4) | 0.320 3(2) |
| B(9) | 0.312 2(3) | −0.210 5(4) | 0.413 2(2) |
| B(10) | 0.189 7(3) | −0.195 4(3) | 0.436 1(2) |
| B(11) | 0.084 2(2) | −0.224 8(3) | 0.360 1(2) |
| B(12) | 0.204 4(3) | −0.308 7(3) | 0.373 0(2) |

## Acknowledgements

A generous loan of palladium salts from Johnson Matthey plc is gratefully acknowledged by T. R. S. G. F. thanks the Natural Sciences and Engineering Research Council (Canada) for Grants in Aid of Research. J. D. K. thanks Dr. X. L. R. Fontaine for assistance with the NMR spectroscopy in the early stages of this work and the SERC for facilities. M. McG. thanks the Department of Education of the Republic of Ireland for a Senior Studentship.

**Table 7** Positional parameters and their estimated standard deviations for [2-$(O_2CMe)$-2-$(PPh_3)$-*closo*-2,1-$PdTeB_{10}H_9(PPh_3)$]·0.79$CH_2Cl_2$ **14**·0.79$CH_2Cl_2$

| Atom | $x$ | $y$ | $z$ | Atom | $x$ | $y$ | $z$ |
|---|---|---|---|---|---|---|---|
| Te | 0.079 41(3) | 0.039 19(2) | 0.123 86(2) | C(44) | 0.443 3(5) | −0.120 8(5) | −0.109 9(3) |
| Pd | 0.160 82(3) | −0.191 98(2) | 0.184 95(1) | C(45) | 0.535 8(5) | −0.213 8(6) | −0.067 9(3) |
| P(1) | 0.071 65(9) | −0.296 95(8) | 0.373 10(4) | C(46) | 0.498 4(5) | −0.273 4(5) | −0.001 4(3) |
| P(2) | 0.312 8(1) | −0.313 83(8) | 0.114 30(4) | C(51) | 0.233 5(4) | −0.411 8(3) | 0.091 4(3) |
| O(1) | −0.001 0(3) | −0.245 7(2) | 0.161 9(1) | C(52) | 0.175 5(4) | −0.478 4(4) | 0.148 5(2) |
| O(2) | −0.031 2(3) | −0.120 4(3) | 0.052 9(2) | C(53) | 0.124 4(5) | −0.558 8(4) | 0.135 1(3) |
| C(A1) | −0.056 9(4) | −0.200 1(3) | 0.102 0(2) | C(54) | 0.126 1(5) | −0.574 5(4) | 0.063 6(3) |
| C(A2) | −0.171 5(5) | −0.242 3(5) | 0.088 6(3) | C(55) | 0.180 3(5) | −0.509 2(4) | 0.007 1(2) |
| C(11) | −0.108 4(4) | −0.276 5(3) | 0.380 6(2) | C(56) | 0.234 3(4) | −0.426 2(4) | 0.019 6(2) |
| C(12) | −0.176 5(4) | −0.288 3(4) | 0.449 2(2) | C(61) | 0.472 7(4) | −0.417 5(3) | 0.152 5(2) |
| C(13) | −0.313 7(5) | −0.276 5(5) | 0.452 9(3) | C(62) | 0.515 2(5) | −0.534 2(4) | 0.147 6(2) |
| C(14) | −0.385 3(5) | −0.250 2(4) | 0.388 9(3) | C(63) | 0.643 4(5) | −0.608 8(4) | 0.173 1(2) |
| C(15) | −0.317 7(4) | −0.241 8(4) | 0.322 3(3) | C(64) | 0.726 9(5) | −0.570 2(4) | 0.204 0(3) |
| C(16) | −0.180 2(4) | −0.253 0(3) | 0.316 6(2) | C(65) | 0.685 2(5) | −0.455 3(5) | 0.210 1(3) |
| C(21) | 0.128 6(4) | −0.309 9(3) | 0.464 1(2) | C(66) | 0.559 9(4) | −0.378 5(4) | 0.184 5(2) |
| C(22) | 0.226 4(5) | 0.408 3(4) | 0.500 4(2) | B(3) | 0.292 6(5) | −0.078 1(4) | 0.177 6(2) |
| C(23) | 0.271 4(7) | −0.411 3(6) | 0.568 3(3) | B(4) | 0.206 8(6) | 0.076 3(4) | 0.201 9(3) |
| C(24) | 0.220 2(6) | −0.316 2(5) | 0.599 0(2) | B(5) | 0.029 9(5) | 0.084 9(4) | 0.236 7(3) |
| C(25) | 0.123 4(6) | −0.221 8(4) | 0.565 9(2) | B(6) | −0.000 7(5) | −0.060 4(4) | 0.237 7(3) |
| C(26) | 0.072 1(5) | −0.214 5(4) | 0.497 3(2) | B(7) | 0.290 8(4) | −0.186 0(4) | 0.268 5(3) |
| C(31) | 0.148 5(4) | −0.439 8(3) | 0.353 4(2) | B(8) | 0.317 9(5) | −0.047 4(4) | 0.262 7(2) |
| C(32) | 0.072 5(4) | −0.515 8(3) | 0.356 7(2) | B(9) | 0.165 6(5) | 0.048 5(4) | 0.296 5(3) |
| C(33) | 0.136 4(5) | −0.626 8(4) | 0.343 4(3) | B(10) | 0.043 6(5) | −0.029 7(4) | 0.318 9(3) |
| C(34) | 0.274 1(6) | −0.664 7(4) | 0.328 7(3) | B(11) | 0.121 9(4) | −0.172 7(3) | 0.302 4(2) |
| C(35) | 0.349 8(5) | −0.590 5(4) | 0.324 9(3) | B(12) | 0.218 9(4) | −0.104 4(4) | 0.336 7(2) |
| C(36) | 0.287 8(4) | −0.478 5(3) | 0.336 5(2) | Cl(1)* | 0.628 2(3) | 0.131 3(2) | 0.312 3(2) |
| C(41) | 0.367 8(4) | −0.238 3(3) | 0.026 2(2) | CS(1)* | 0.621(11) | 0.034 0(8) | 0.389 1(7) |
| C(42) | 0.273 3(5) | −0.143 6(4) | −0.016 4(2) | Cl(2)* | 0.659 4(3) | 0.045 8(3) | 0.471 5(2) |
| C(43) | 0.313 1(5) | −0.085 2(5) | −0.085 5(2) | | | | |

* Site occupancy factor is 0.79.

## References


1 Part 10, S. Coughlan, T. R. Spalding, G. Ferguson, J. F. Gallagher, A. J. Lough, X. L. R. Fontaine, J. D. Kennedy and B. Štibr, *J. Chem. Soc., Dalton Trans.*, 1992, 2865.
2 G. Ferguson, M. Parvez, J. A. MacCurtain, O. Ni Dhubhghaill, T. R. Spalding, G. Ferguson, B. Kaitner, X. L. R. Fontaine and J. D. Kennedy, *J. Chem. Soc., Dalton Trans.*, 1987, 699.
3 Faridoon, O. Ni Dhubhghaill, T. R. Spalding, G. Ferguson, B. Kaitner, X. L. R. Fontaine and J. D. Kennedy, *J. Chem. Soc., Dalton Trans.*, 1989, 1657.
4 G. Ferguson, J. D. Kennedy, X. L. R. Fontaine, Faridoon and T. R. Spalding, *J. Chem. Soc., Dalton Trans.*, 1988, 2555.
5 Faridoon, O. Ni Dhubhghaill, T. R. Spalding, G. Ferguson, B. Kaitner, X. L. R. Fontaine, J. D. Kennedy and D. Reed, *J. Chem. Soc., Dalton Trans.*, 1988, 2739.
6 S. K. Boocock, N. N. Greenwood and J. D. Kennedy, *J. Chem. Soc., Chem. Commun.*, 1980, 305.
7 S. K. Boocock, N. N. Greenwood, J. D. Kennedy, W. S. McDonald and J. Staves, *J. Chem. Soc., Dalton Trans.*, 1981, 2573.
8 S. R. Bunkhall, X. L. R. Fontaine, N. N. Greenwood, J. D. Kennedy and M. Thornton-Pett, *J. Chem. Soc., Dalton Trans.*, 1990, 73.
9 T. B. Marder, R. T. Baker, J. A. Long, J. A. Doi and M. F. Hawthorne, *J. Am. Chem. Soc.*, 1981, **103**, 2988.
10 H. J. Gysling, H. R. Luss and D. L. Smith, *Inorg. Chem.*, 1979, **18**, 2696.
11 H. M. Colquhoun, T. J. Greenhough and M. G. H. Wallbridge, *J. Chem. Soc., Dalton Trans.*, 1985, 761.
12 D. A. Redfield and J. H. Nelson, *Inorg. Chem.*, 1973, **12**, 15.
13 J. A. Ruhn, D. J. O'Donnell, A. R. Palmer and J. H. Nelson, *Inorg. Chem.*, 1989, **28**, 2631.
14 G. R. Newkome, W. E. Puckett, G. E. Kiefer, V. K. Gupta, F. R. Fronczek, D. C. Pantaleo, G. L. McClure, J. B. Simpson and W. A. Deutsch, *Inorg. Chem.*, 1985, **24**, 811.
15 M. Zocchi, G. Tieghi and A. Albinati, *J. Chem. Soc., Dalton Trans.*, 1973, 883.
16 G. J. Gainsford and R. Mason, *J. Organomet. Chem.*, 1974, **80**, 395.
17 J. Shelbin, K. Abboud and S. F. Watkins, *J. Organomet. Chem.*, 1983, **241**, 259.
18 E. Wehman, G. van Koten, J. T. B. H. Jastrzebski, H. Ossor and M. Pfeffer, *J. Chem. Soc., Dalton Trans.*, 1988, 2975.
19 J. D. Kennedy, *Prog. Inorg. Chem.*, 1984, **32**, 519; 1986, **34**, 211.
20 J. R. Blackburn, R. Nordberg, F. Stevie, R. G. Albridge and M. M. Jones, *Inorg. Chem.*, 1970, **9**, 2374.
21 J. M. Jenkins and B. L. Shaw, *J. Chem. Soc. A*, 1966, 770.
22 J. L. Little, G. D. Friesen and L. J. Todd, *Inorg. Chem.*, 1977, **16**, 869.
23 SDP-PLUS Program system, B. A. Frenz and Associates, College Station, TX and Enraf-Nonius, Delft, 1983.
24 G. Sheldrick, SHELX 76, A program for crystal structure analysis, University of Cambridge, 1976.
25 N. Walker and D. Stewart, *Acta Crystallogr., Sect. A*, 1983, **39**, 158.
26 *International Tables for X-Ray Crystallography*, Kynoch Press, Birmingham, 1974, vol. 4.
27 C. K. Johnson, ORTEP II, Report ORNL-5138, Oak Ridge National Laboratory, TN, 1976.
28 E. J. Gabe, Y. LePage, J. P. Charland, F. L. Lee and P. S. White, *J. Appl. Crystallogr.*, 1989, **22**, 384.


*Received* 19*th May* 1992; *Paper* 2/02610D